



**ORGANISATION EUROPEENNE POUR LA RECHERCHE NUCLEAIRE  
EUROPEAN ORGANIZATION FOR NUCLEAR RESEARCH**

*Laboratoire Européen pour la Physique des Particules  
European Laboratory for Particle Physics*

TECHNICAL NOTE

CERN-SC-2004-23-RP-TN

**SIMULATION AND EXPERIMENTAL VERIFICATION OF THE RESPONSE  
FUNCTIONS OF CENTRONIC HIGH-PRESSURE IONISATION CHAMBERS**

Christian Theis, Markus Rettig, Stefan Roesler and Helmut Vincke

**Abstract**

In the course of designing a radiation monitoring system for the LHC it is necessary to study the response functions of different monitoring devices thoroughly in order to identify suitable candidates. Among the systems currently investigated are IG5 ionisation chambers by Centronic Ltd. Generally, Monte Carlo simulations are a suitable tool to investigate the response to specific particle types over a wide energy range and also to mixed radiation fields. This note describes the simulations performed using the FLUKA particle transport code to calculate response functions for argon- and hydrogen-filled IG5 chambers with respect to various particle types at different energies. The results obtained for photons and neutrons are also compared to measurements that were performed to validate the simulation model.

CERN, Geneva, Switzerland

30.06.2004

## 1 INTRODUCTION

For the Large Hadron Collider (LHC) it is in the responsibility of the Radiation Monitoring System for the Environment and Safety (RAMSES) project to implement a system for radiological surveillance. In order to ensure accurate measurements of dose rates it is of great importance to investigate the response of potential candidates for monitoring devices thoroughly, especially with respect to the mixed field composition encountered at a high-energy accelerator.

It is foreseen to install ionisation chambers in areas where dose is due to radiation fields consisting of neutrons, photons and charged particles. Presently argon- and hydrogen-filled IG5 ionisation chambers, supplied by Centronic Ltd.<sup>1</sup>, are used at the Super Proton Synchrotron (SPS) and its respective experimental areas. Hence, it is of interest to investigate whether this specific type of chamber can serve its function well enough to be used as a radiation monitor for the LHC. The calibration factor for these devices is typically determined using photon and neutron calibration sources. However, the response in an environment with a deviating energy spectrum and particle population can be different and is poorly understood so far. Therefore, Monte Carlo simulations are necessary to investigate their response to specific particle types over a wide energy range and also to mixed radiation fields.

Preliminary studies of the response of these chambers to gamma and neutron radiation have already been performed with the FLUKA particle interaction and transport code [1,2] using a simple geometric model [3]. Results were benchmarked with X-ray, Am-241, Cs-137 and Co-60 sources at CERN's calibration laboratory and at the Paul Scherrer Institute (PSI) [4]. This Note discusses the results of the simulations obtained with a more detailed model of the chambers. Furthermore, the response to neutrons as well as to other particles commonly encountered in a mixed radiation field, like protons, muons, pions and electrons has been investigated extensively. The experimental verification of these results, as performed in the mixed radiation field of the CERN-EU high-energy Reference Field (CERF) facility [5] and with mono-energetic neutron beams at the Physikalisch-Technische-Bundesanstalt Braunschweig (PTB), is currently under study.

## 2 THE FLUKA SIMULATION

All calculations were carried out using the 2002 version of the Monte-Carlo code FLUKA, see [1,2] and references they contain.

### 2.1 GEOMETRY OF THE CHAMBER

The geometry of the IG5 chamber was obtained from drawings and information supplied by the manufacturer. Sections through the geometrical model as implemented in the FLUKA simulations are shown in Figure 1. The monitor consists of a cylindrical steel shell with a spherical head. It contains two similarly shaped electrodes which delimit an

---

<sup>1</sup> Centronic Limited, Centronic House, Croydon CR9 0BG, England

active volume of 5.2 l filled with argon or hydrogen pressurised at 20 bar. The bottom of the chamber is sealed by a base plate, with a cylindrical steel case attached to it, containing an electronics board for power supply and signal processing.

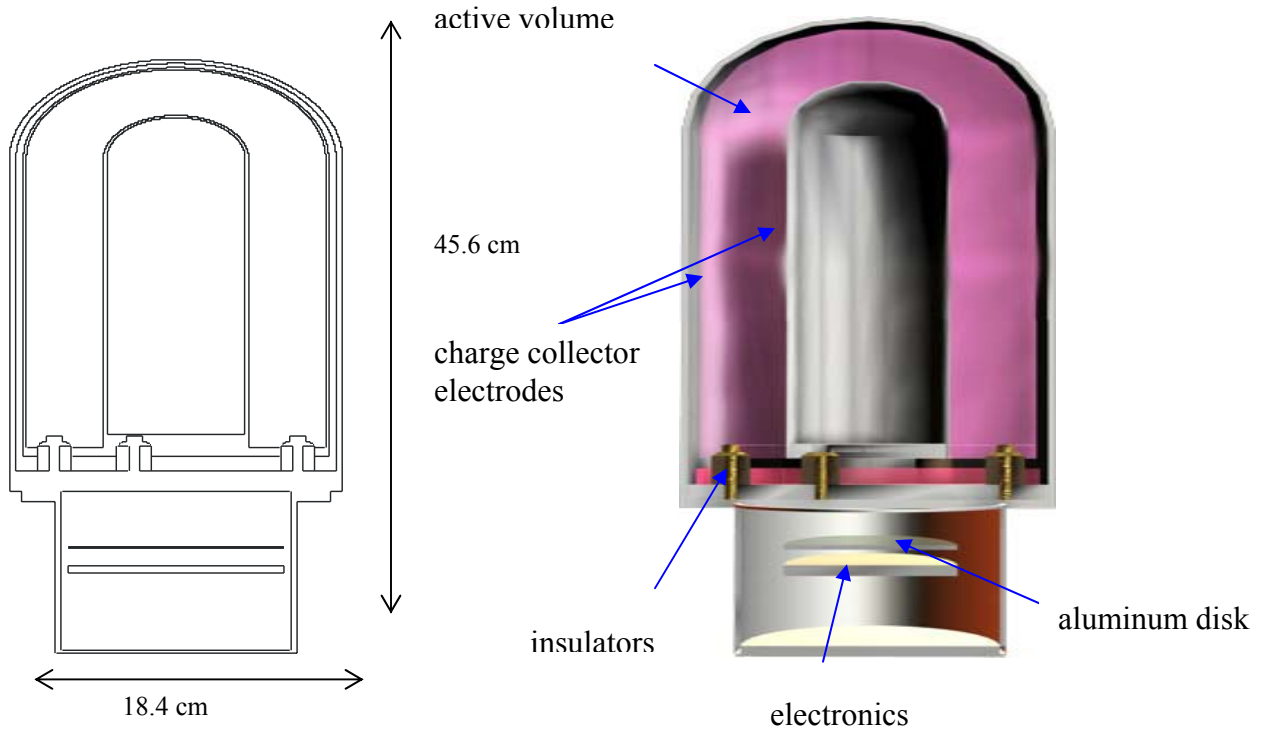


**Figure 1** Geometry of the IG5 ionisation chamber as used in the FLUKA simulations.

The shell of the chamber is made of mild steel. The exact material composition was not available from the manufacturer and thus typical values from material databases [6] (99.5% iron and 0.5% carbon) have been adopted. However, it should be noted mild steel is available on the market with different elemental compositions. Due to the fact that the electronics board inside the steel case could not be modelled accurately, it was approximated using an average elemental composition of 35% Si, 2.5% C, 2.5% Cu, and 60% epoxy resin distributed uniformly over a disc of 5.933 cm radius, 0.67 cm height and a density of 1.95 g/cm<sup>3</sup>. The latter was calculated from the weight of the board which was measured to be 144.95 g.

## 2.1 SIMULATION PARAMETERS

The cascade simulations were based on a detailed treatment of the hadronic and electromagnetic shower induced in the chamber by a parallel beam of mono-energetic particles of a certain type. Studied beam particles comprised electrons, photons, neutrons, protons, positively and negatively charged pions as well as muons. The comparison of simulation results to measurements using X-ray sources is an exception, as in this case the energy of the beam particle (X-ray) was sampled from standardized distributions (*c.f.* Section 3).

The beam spot was chosen to be annular with a radius of 22.63 cm. Unless stated otherwise lateral irradiation, perpendicular to the symmetry axis of the chamber, was assumed. Secondary hadrons were transported until they were stopped or captured, including thermal energies for neutrons. The electromagnetic cascade was simulated in detail down to kinetic energy thresholds of 200 keV and 10 keV for electrons/positrons and photons, respectively.

Energy deposition in the active volume is the primary quantity calculated with FLUKA. The produced charge is then deduced by dividing this value by the average energy necessary to produce an ion pair, the so-called  $W$ -factor. Because of other occurring processes like excitation, the average energy lost in an energy deposition event is substantially greater than the ionisation energy. However, this is taken into account in the definition of the  $W$ -factor. In principle, its value is a function of the gas, the type of radiation and its energy. However, empirical observations have shown that it does not show a strong dependence on energy and particle type, hence, can be approximated in most cases by a constant value for the respective gas type [7,8].

For the charged particles that were investigated, such as pions, electrons and muons, the same values as for photons were adopted. According to [7] the dependence of the  $W$ -factor on the particle type is in most cases of minor importance for one specific gas type. However, the processes arising from neutron irradiation are more subtle. In this case no unique  $W$ -factor exists because its value strongly depends on the interaction processes involved, which in turn are determined by the type of gas used as an active medium. The predominant interaction process in case of hydrogen gas is proton recoil. On the other hand neutron interaction with argon might cause, *e.g.*, the nucleus to recoil or trigger the emission of other secondary particles causing ionization. Following the approach chosen for the preliminary studies [3] the  $W$ -factor for proton recoil was adopted for both gases for neutron and proton irradiation. However, it should be kept in mind that this simplification might contribute to deviations of the calculated response from measured values.

All values of the  $W$ -factor used in this study are summarised in Table 1. Taking the area of the annular beam spot into account, the sensitivity of the chamber is obtained in terms of charge per unit fluence. By dividing this value by the appropriate fluence to dose equivalent conversion factor [9,10] the response can be expressed in terms of charge per unit dose equivalent.

**Table 1** Average energy needed to produce an ion pair ( $W$ -factor) taken from [7]. Values are given for two source particle types and argon and hydrogen gases. For charged particles such as pions, muons and electrons the same values as for photons were adopted.

Source particle	Argon	Hydrogen
Photon	26.40 eV	36.50 eV
Neutron, Proton	26.66 eV	36.43 eV

### 3 RESPONSE TO PHOTONS

Using FLUKA response calculations for photons ranging from 48 keV (average energy of the ISO standard N60 X-ray spectrum, see Table 2 and Figures 4 and 5) up to 10 MeV were performed for argon- and hydrogen-filled chambers. The results expressed in terms of created charge per unit fluence are illustrated in Figure 2.

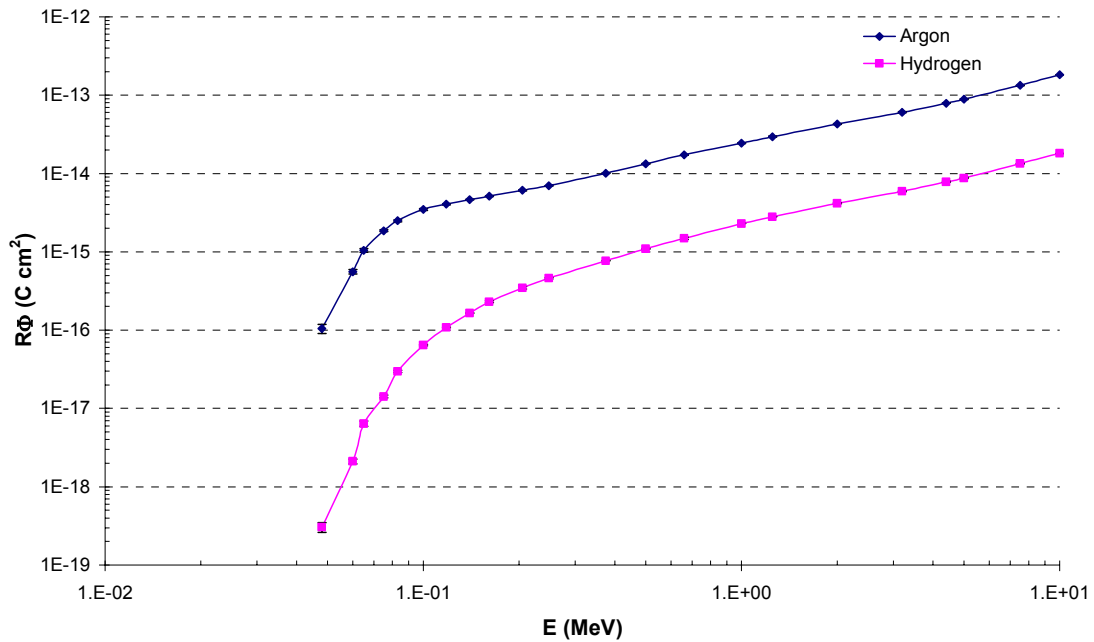


**Figure 2** *Calculated response to photons, expressed in terms of created charge per unit fluence, for argon- and hydrogen-filled IG5 chambers.*

In order to compare the results of the simulation to the measurements (given in charge per air-kerma) discussed in [4] it is necessary to apply appropriate dose conversion factors (see Appendix). In the case of photons, fluence-to-air kerma conversion coefficients were used, as calibration fields are typically characterised in terms of kerma in air. Consequently, the response is expressed in terms of created charge per unit kerma.

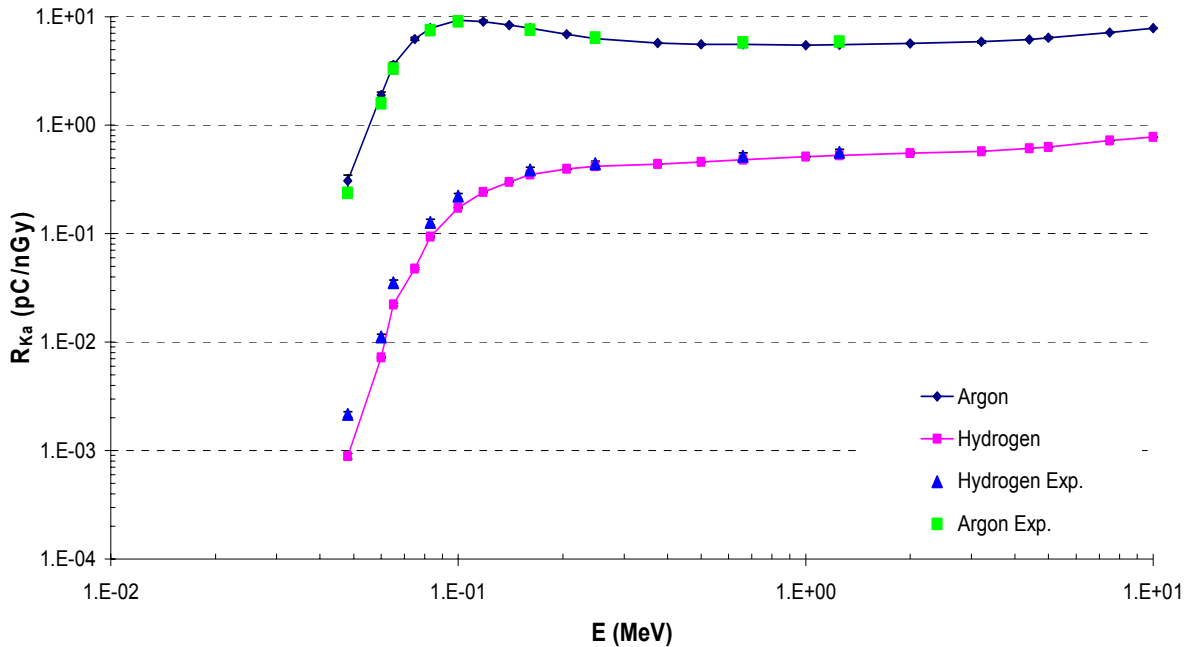


**Figure 3** *Calculated response to photons expressed in terms of created charge per energy released in matter for argon- and hydrogen-filled IG5 chambers. In addition values measured with different calibration sources are shown.*

As can be seen from Figure 3 the argon-filled chambers are more sensitive to photon irradiation than the hydrogen-filled devices by a factor of approximately 10. In order to verify the simulation results the measured data, obtained with the respective calibration sources, are also shown in Figure 3. For most values the comparisons show good agreement of the simulated and the experimental values within statistical uncertainties of the measurements, which were obtained by repetition of the experiments with different monitors of each type.

It should be noted that the experimental result for 60 keV as well as for the two values of highest energy were obtained with standard calibration sources Am-241 (60 keV), Cs-137 (660 keV) and Co-60 (1.17 MeV and 1.33 MeV, the response is shown for the average energy of 1.25 MeV), whereas responses for the other energies were measured with X-ray sources at the Paul Scherrer Institute (PSI) [4]. For the latter measurements the sources given in Table 2 were used. In the earlier studies [4] simulations were performed only for the mean energy of the respective spectra, which resulted in an expected deviation from the experimental values. In order to study this effect the calculations were repeated with the refined geometrical model of the chamber using only mono-energetic photons of the respective mean energies and also actual energy spectra [11] (see Figures 4 and 5).

**Table 2** ISO identification and mean energy of the X-ray sources that were used for calibration measurements. The respective abbreviations will be used throughout this note.

ISO radiation quality	Mean photon energy [keV]
N60	47.9
N80	65.2
N100	83.3
N120	100.4
N200	164.8
N300	248.4

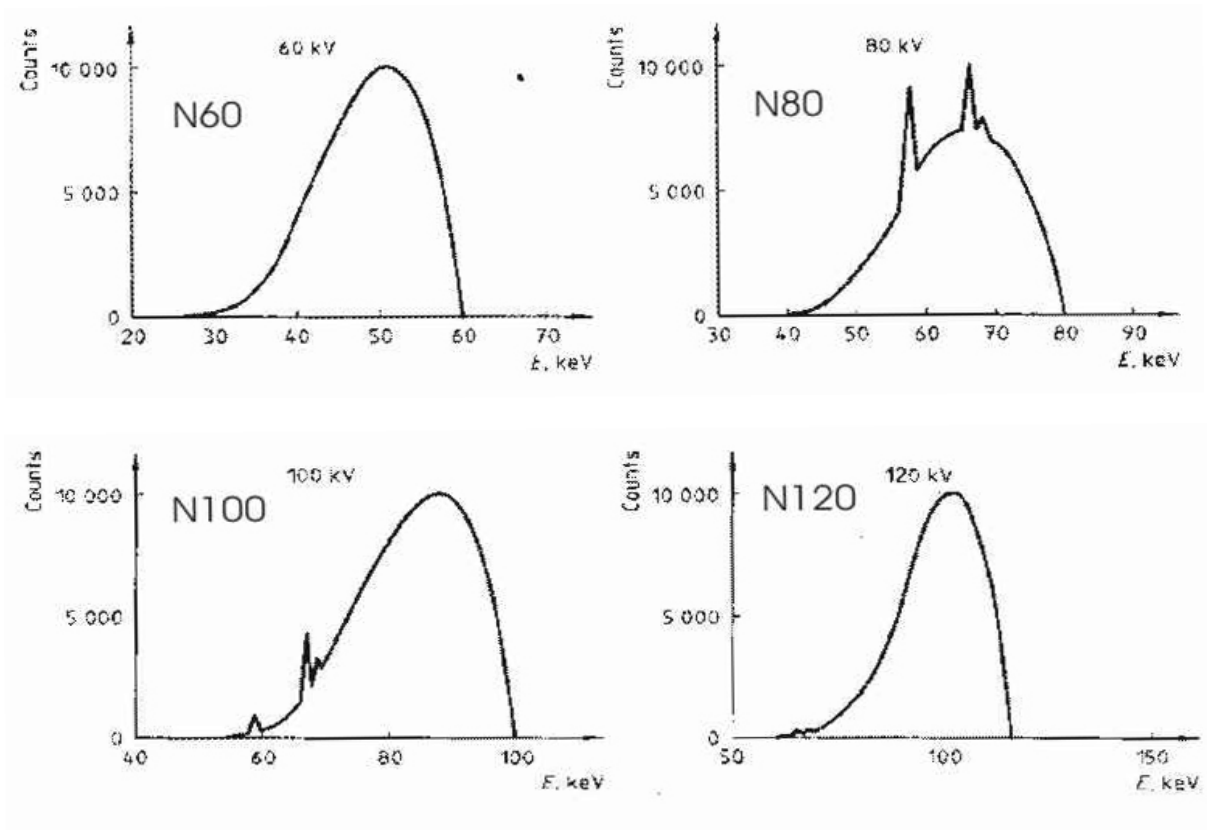


**Figure 4** Energy spectra of various standardized X-ray sources used in the simulations.

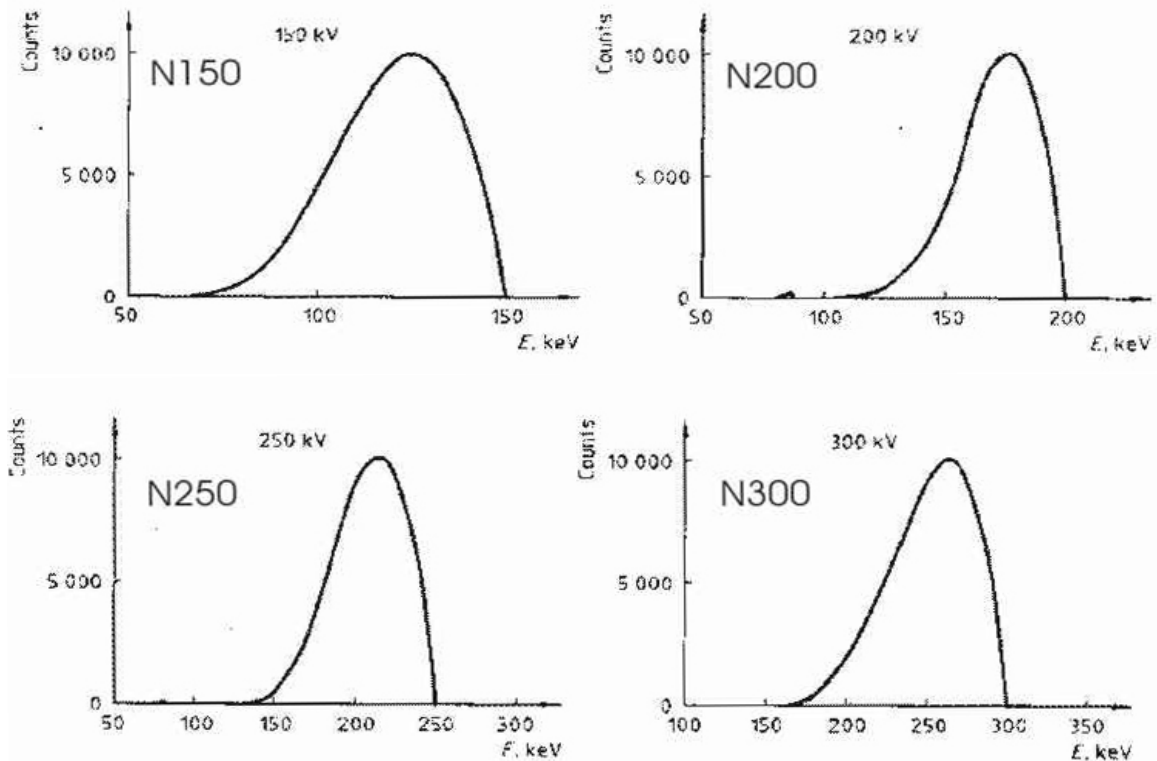


**Figure 5** Energy spectra of the standardized X-ray sources used in the simulations, with the exception of radiation qualities N150 and N250.

Table 3 shows the ratio of the simulated response and the measured values using either the mean energy or the actual energy spectrum for the argon-filled chamber.

**Table 3** Ratio of the simulated response of an argon-filled chamber and the corresponding measured values using either a mono-energetic photon beam or the actual X-ray spectra.

ISO radiation quality	Ratio (spectrum)	Ratio (mean energy)
N60	$1.29 \pm 14\%$	$0.37 \pm 11\%$
N80	$1.08 \pm 7\%$	$0.83 \pm 5\%$
N100	$1.05 \pm 5\%$	$0.98 \pm 5\%$
N120	$1.03 \pm 5\%$	$1.00 \pm 5\%$
N200	$1.03 \pm 5\%$	$1.01 \pm 5\%$
N300	$1.06 \pm 5\%$	$1.04 \pm 5\%$

As can be seen, sampling the energies from actual spectra improves the agreement of the simulation with respect to the measured data, especially for the sources N60 and N80. However, a slightly higher response can be observed in the simulation especially for low-energy photons. An explanation of this effect could be a possible deviation in the assumed composition of the mild steel used for the chamber hull. Especially in the case



of low-energy photon irradiation a corresponding uncertainty in the material composition of the shell might contribute significantly to a discrepancy between measurement and simulation results.

The geometry specification supplied by the producer included an uncertainty regarding the thickness  $d_0$  of the steel shell ( $d_0 = 3.455 \text{ mm} \pm 5\%$ ). Especially in the case of irradiation with low-energy photons the margin on this value is expected to have a strong influence on the response. Therefore, it was decided to include this in the uncertainty of the calculated response after performing a more detailed analysis. In order to determine the influence on the energy deposition in the active volume simulations were performed for two different thicknesses. These values were chosen based on the assumption that the uncertainty of 5%, given by the manufacturer, is uniformly distributed with a mean of  $d_0 = 3.455 \text{ mm}$ , resulting in a standard deviation  $\sigma = 9.974 \times 10^{-2} \text{ mm}$ . Thus, the two values, which were selected corresponding to  $d_0 \pm \sigma$ , are  $d_1 = 3.355 \text{ mm}$  and  $d_2 = 3.555 \text{ mm}$ . Energy deposition was calculated for chambers of corresponding wall thicknesses using mono-energetic photon beams of 60 keV and 1250 keV, respectively. As a result for a beam energy of 60 keV a relative deviation of 6.36% was obtained with respect to calculations assuming a wall thickness of  $d_0$ . On the other hand at 1250 keV the deviation is within the statistical error of the calculation, whereas at lower energies a significant effect can be observed. Similar calculations would have to be conducted for all energies used for the simulation calculation of the response functions. Due to the fact that performing such Monte Carlo simulations is quite a CPU-time consuming task it was necessary to find a fast and suitable method to obtain an estimate of the influence. Using exponential attenuation  $e^{-(\mu \cdot \sigma \cdot \rho)}$ , with  $\mu$  being the mass energy absorption coefficient,  $\sigma$  the deviation of the thickness from its expected value  $d_0$  and  $\rho$  the density of the steel shell ( $\rho = 7.8 \text{ g/cm}^3$ ), one obtains a relative deviation of 6.49% for a beam energy of 60 keV. This result matches the value obtained from the Monte Carlo simulation within statistical deviations. Hence, the contribution to the errors originating from possible variations of the wall-thickness was calculated accordingly for all energies that were considered for response calculations.

## 4 RESPONSE TO NEUTRONS

### 4.1 FLUKA CALCULATIONS

At the LHC the major contribution to the expected dose outside the shielding is caused by neutrons. Hence, it is of great importance to have good knowledge of the response of the chambers to these particles within the expected energy range. Depending on the particle energy interactions are described within FLUKA by different models. Hadron - nucleus interactions at energies above 4 GeV are treated according to the Dual Parton Model (DPM). In the energy range between 3.5 GeV and 4-5 GeV resonance production and decay models are applied. Processes below are handled by the Generalized Intranuclear Cascade (GINC) model, including the treatment of evaporation, fission, Fermi break-up and  $\gamma$ -excitation. FLUKA's implementation of the GINC formalism for energies from 3.5 GeV down to the reaction threshold is called PreEquilibrium Approach to Nuclear Thermalization (PEANUT) model [2].

In the case of neutrons elastic and inelastic reactions below 19.6 MeV are simulated based on tabulated cross-sections. Consequently, the energy range from  $1.0 \times 10^{-11}$  MeV up to 19.6 MeV is divided into 72 energy intervals (groups) for which cross-sections are available for about 140 materials. Additionally, cross-section sets for neutron induced  $\gamma$  - reactions are supplied in a 22 energy-group structure covering a range from 10 keV to 20 MeV. For most materials, with the exception of hydrogen, the calculation of energy deposition in the respective material is based on kerma factors. As a consequence the average value of energy deposited is the same for each neutron interaction within one of the 72 groups. However, considering the large amount of particles transported in the simulation the use of a group structure approximation is expected to have a minor influence on the result in many cases, at the advantage of gaining computation speed.

Similar to the calculations for photons the energy deposition in the active volume was calculated for neutrons with energies ranging from thermal energy ( $1 \times 10^{-21}$  eV) up to 5 GeV. The upper limit was chosen to lie above the expected threshold of significant neutron contribution at accessible areas of the LHC. Below 19.6 MeV the binning in the response function corresponds to the energy binning of the low-energy neutron cross-sections. The response function, expressed in terms of charge per unit fluence, is then obtained by dividing the energy deposition by the appropriate  $W$ -factor (see Table 1) and subsequent multiplication with the unit charge. The results are illustrated in Figure 6.

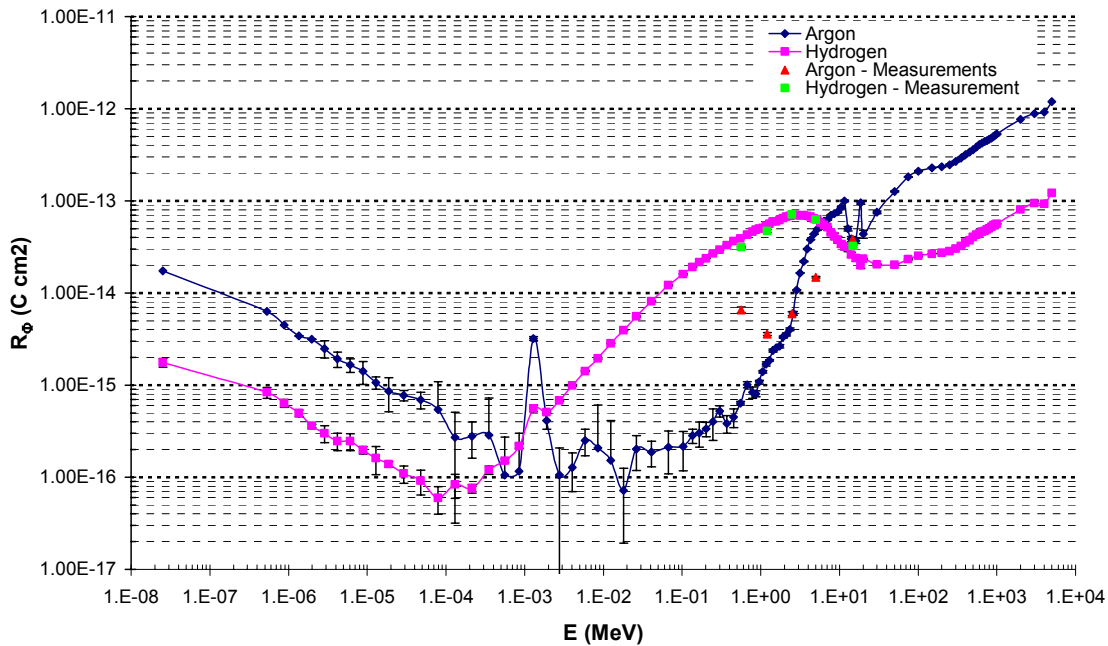


**Figure 6** Neutron response expressed in terms of created charge per unit fluence for argon- and hydrogen-filled IG5 chambers. Calculated values are connected by a constrained cubic spline fit.

Furthermore, by multiplying these values with fluence-to-ambient dose equivalent conversion factors [10] (see Appendix) response can be expressed in terms of charge per unit dose equivalent. The resulting energy dependence is shown in Figure 7.

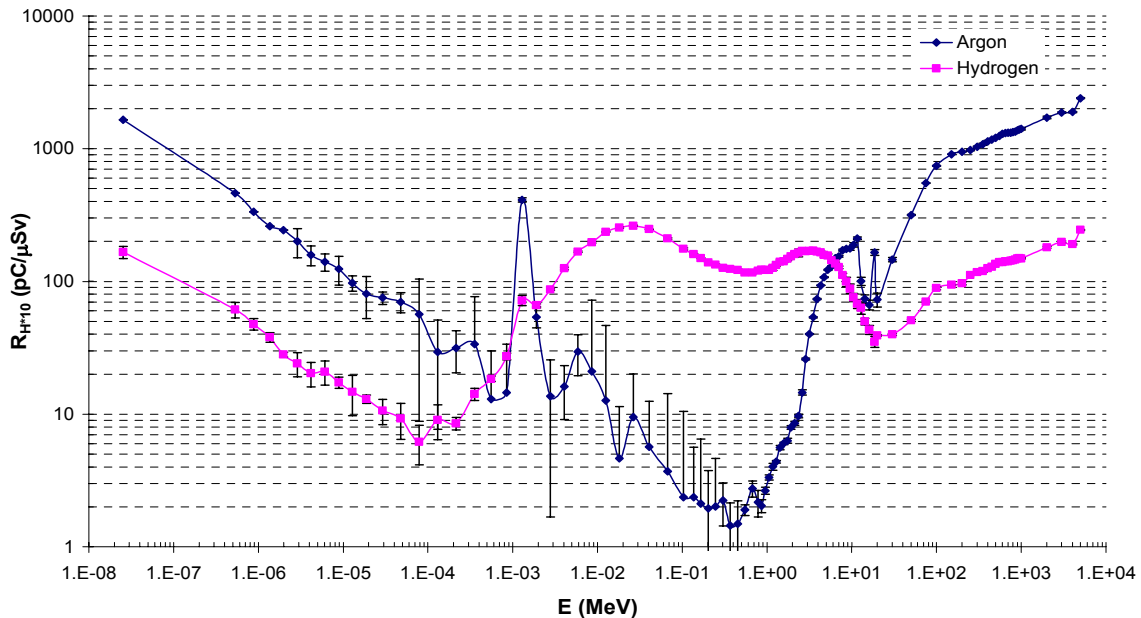


**Figure 7** Calculated response functions for neutrons expressed in terms of created charge per unit ambient dose equivalent for argon- and hydrogen-filled IG5 chambers.

As expected, for neutrons ranging from 1 keV up to 10 MeV the response of an argon-filled chamber is significantly lower than that of a hydrogen-filled device, as the latter has a higher neutron scattering cross section and a more efficient energy transfer can be observed due to the comparable masses of the incident particle and the hydrogen nucleus. The peak in the response of the argon-filled chamber for the cross-section group with an average energy of 1.29 keV can be explained by the iron content of the chamber wall, which in turn has a rather high probability for a (n, $\gamma$ ) process at this specific energy. As can be seen from Figure 6 and Figure 7 above 50 MeV the response of argon-filled chambers to neutrons is significantly higher than that of hydrogen-filled monitors. The observed behaviour was subject to further investigation and found to be due to spallation reactions on argon, *e.g.*, knocking off protons which cause the higher response. This would indicate that an argon chamber is a suitable candidate to detect high-energy neutrons. However, one has to keep the significant response of an argon-filled monitor to photons and charged particles in mind (see Figures 3 and 11) and therefore the fact that the device is prone to show a high response to natural background radiation. Consequently, it is always important to perform appropriate corrections for measurements with argon-filled monitors.

#### 4.2 EXPERIMENTAL VERIFICATION

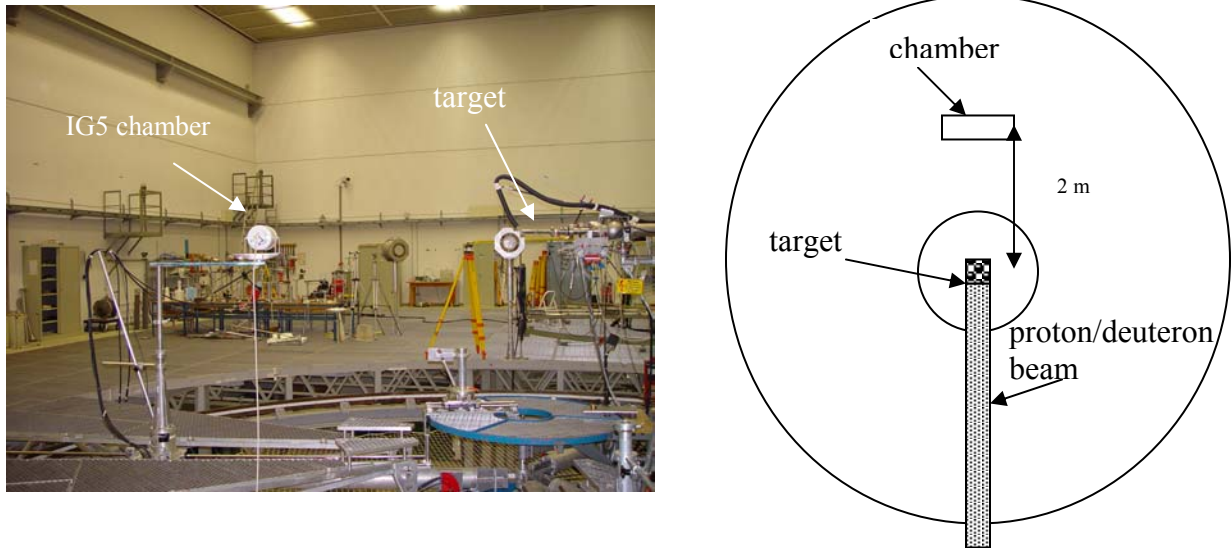
In order to verify the calculated responses to neutrons calibration measurements were performed at the Physikalisch-Technische-Bundesanstalt (PTB) Braunschweig in November 2003, using an argon-filled (Inv. No. 2618) and a hydrogen-filled IG5 ionisation chamber (Inv. No. 112545). The irradiation facility at the PTB provides mono-energetic neutron beams in the energy range from 24 keV up to 19 MeV, produced in interactions of proton or deuteron beams with different targets [13]. In general air cooled LiOH or Ti foils serve as carrier materials, which are coated with a neutron producing layer. Only mono-energetic beams of 5 MeV or 8 MeV are created with gas targets. For the calibration measurements the energies given in

Table 4 were selected.

**Table 4** *Energies and reactions that were selected for neutron calibration measurements. Additionally, the nominal dose rate at the irradiation location of the monitors (2 m distance from the target) and the respective irradiation time is given.*

Energy [MeV]	Reaction	Target ID	Nominal dose rate [mSv/h]	Irradiation time [min] for Ar	Irradiation time [min] for H
0.565	${}^7\text{Li}(p,n){}^7\text{Be}$	LiOH(40)	0.500	195	5
1.2	$\text{T}(p,n){}^3\text{He}$	GU80	0.840	95	5
2.5	$\text{T}(p,n){}^3\text{He}$	GU75	2.020	30	5
5.0	$\text{D}(\text{D},n){}^3\text{He}$	Gas	1.730	5	5
14.8	$\text{T}(\text{D},n){}^4\text{He}$	Al-95-2	6.690	5	5
14.8	$\text{T}(\text{D},n){}^4\text{He}$	Al-95-2	0.700	5	5
14.8	$\text{T}(\text{D},n){}^4\text{He}$	Al-95-2	0.070	15	15
14.8	$\text{T}(\text{D},n){}^4\text{He}$	Al-95-2	0.007	100	100

In the experimental hall the chambers were mounted with the centre of the monitor being placed at a distance of 2 m from the respective target (see Figure 8).



**Figure 8** Experimental setup for the irradiation of the IG5 chambers at the PTB.

Both monitors were exposed to the beam laterally as well as from the head and the rear. Consequently, the results were used to benchmark the simulations of the response functions and the angular dependence (*c.f.* Section 6). All measurements were performed for the selected energies at the highest dose rate available in 2 metres distance. The exposure duration was chosen as such that the total charge created at a certain neutron energy was equivalent to the one created by 14.8 MeV neutrons during 5 minutes of irradiation at a dose rate of 6.69 mSv/h. The respective times were obtained based on the response functions given in Figure 7 and are listed in Table 4.

In order to test the linearity of the response both chambers were exposed to different dose rates at a neutron energy of 14.8 MeV. In addition to the count rate of the IG5 monitors the count rate of the beam monitor, the so called New Monitor (NM), was recorded. Applying a given calibration factor to the latter values one obtains the neutron fluence per  $\text{cm}^2$  at the irradiation location. The measured current of the IG5 monitors irradiated with neutrons of 14.8 MeV is shown as a function of fluence in Figure 9.

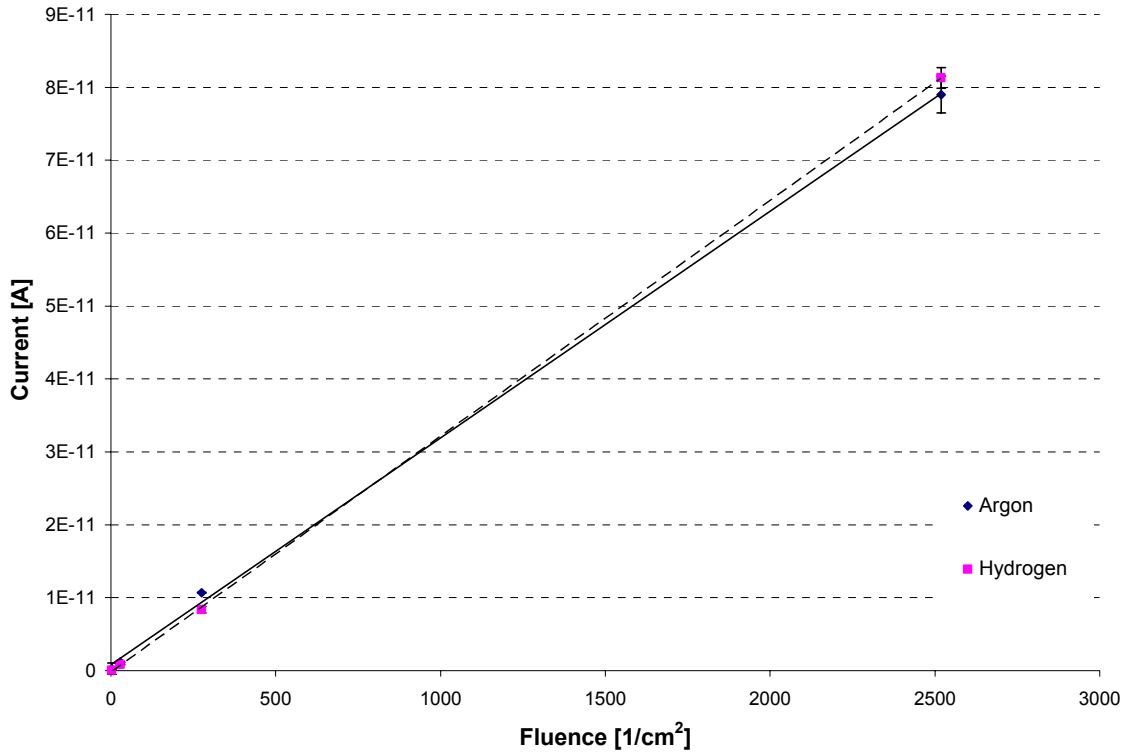


**Figure 9** Measured current as a function of fluence for an argon-filled and a hydrogen-filled IG5 chamber in a mono-energetic neutron field of 14.8 MeV.

Due to the large dimensions (24 m x 30 m x 14 m) of the experimental hall scattering effects from the walls and the floor are expected to have a minor influence. In order to investigate the contribution of scattered low-energy neutrons and photons to the readings of the monitors measurements with so-called shadow-cones were performed at a neutron energy of 2.5 MeV. A cone consisting of iron and polyethylene was placed into the beam in front of the ionisation chamber in order to prevent direct irradiation (see Figure 10).



**Figure 10** Measurement setup with a shadow-cone placed between the target and the chamber to determine the contribution of scattered neutrons to the recorded signal.

As a result the contribution was determined to be about 1% for the hydrogen-filled chamber and 22% for the argon-filled monitor, respectively. Due to the negligible effect of scattered particles on the readings of the hydrogen-filled chamber no background correction was performed in this case. The situation is more complicated for the argon-filled monitor as the chamber is rather sensitive to photons. Thus, photons created in the shadow-cone by neutron interactions might contribute to the readings and the background can therefore not be subtracted unambiguously. Further studies of radiation originating directly from the shadow-cone are necessary (*e.g.*, by simulation) in order to resolve this question.

The measurement results for both chambers are given in Figure 6 in terms of created charge per unit fluence. As can be seen good agreement is found for the hydrogen-filled device, whereas for the argon-filled monitor large deviations can be observed. These discrepancies are not yet fully understood but it is important to keep in mind that the calculated and the measured quantity are different. As a result of the FLUKA simulation one obtains energy deposition. The calculation of this quantity is based on kerma factors for argon, whereas for hydrogen detailed kinematics of elastic scattering on hydrogen nuclei and the transport of recoil protons are implemented. Any occurring process, for example nuclear interactions, expending deposited energy but not directly resulting in ionization, might contribute to possible deviations in comparison to the measured charge, if it is not correctly taken into account by the conversion to the number of formed ion pairs. Further investigations of this matter have to be performed.

## **5 RESPONSES TO CHARGED PARTICLES**

The typical composition of a mixed radiation field outside the shielding of a high-energy accelerator also includes charged particles, such as muons, pions, protons and electrons. Thus, the responses of the two types of chambers to these particle types have been calculated and results are illustrated in Figure 11 - Figure 14. For reasons of comparison the response to neutrons is also shown in the figures.

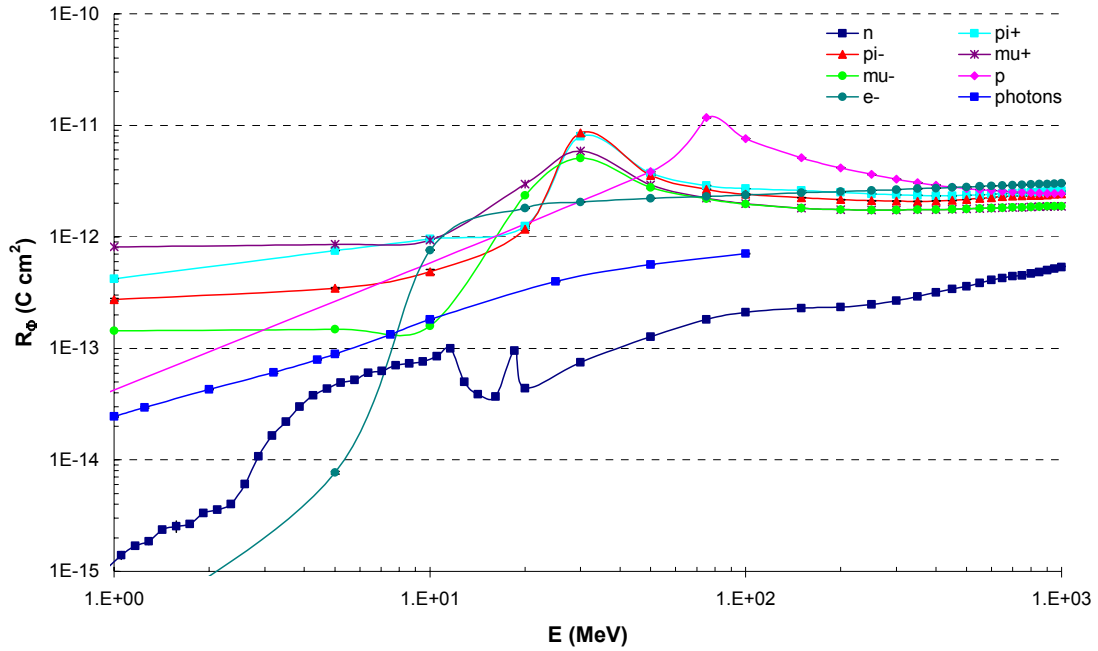


**Figure 11** Response functions for protons, neutrons, muons, charged pions and electrons expressed in terms of created charge per unit fluence for an argon-filled IG5 chamber. Calculated values are connected by a constrained cubic spline fit.

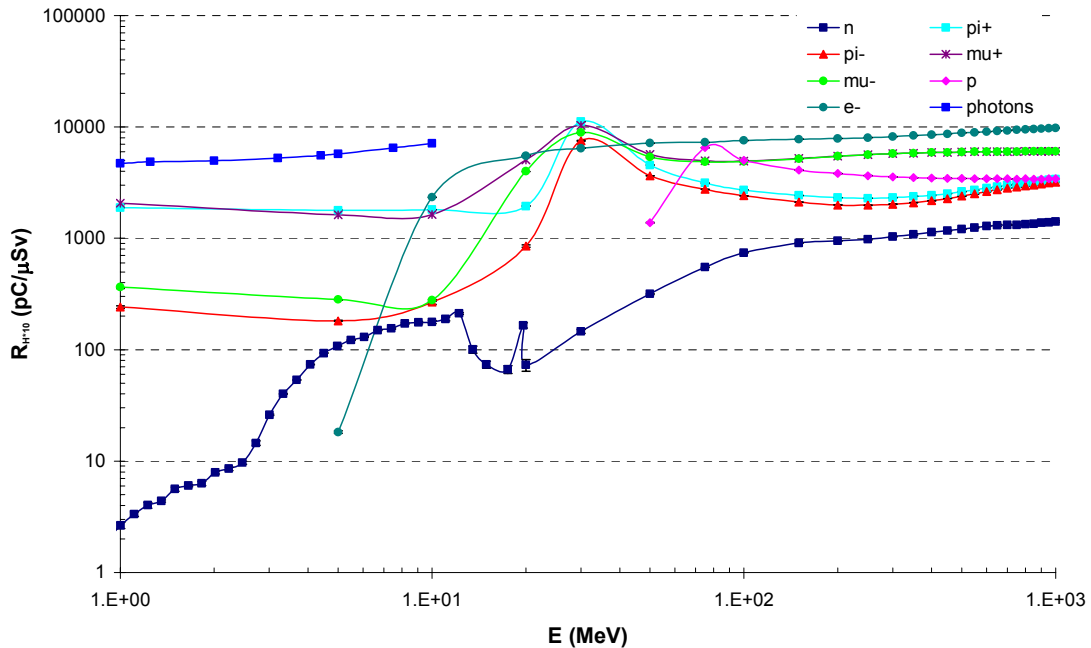


**Figure 12** Response functions for protons, neutrons, muons, charged pions and electrons expressed as created charge per unit dose equivalent for an argon-filled IG5 chamber. Conversion coefficients for electron energies below 2 MeV and for proton energies below 50 MeV were not available from [10].



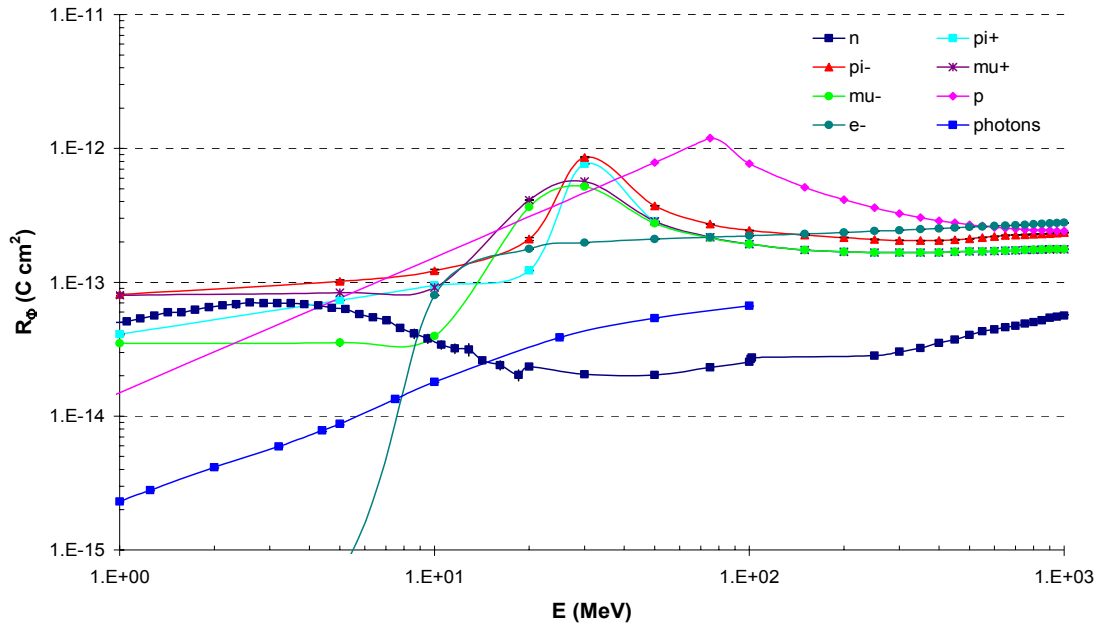


**Figure 13** Response functions for protons, neutrons, muons, charged pions and electrons expressed in terms of created charge per unit fluence for a hydrogen-filled IG5 chamber. Calculated values are connected using a constrained cubic spline fit.

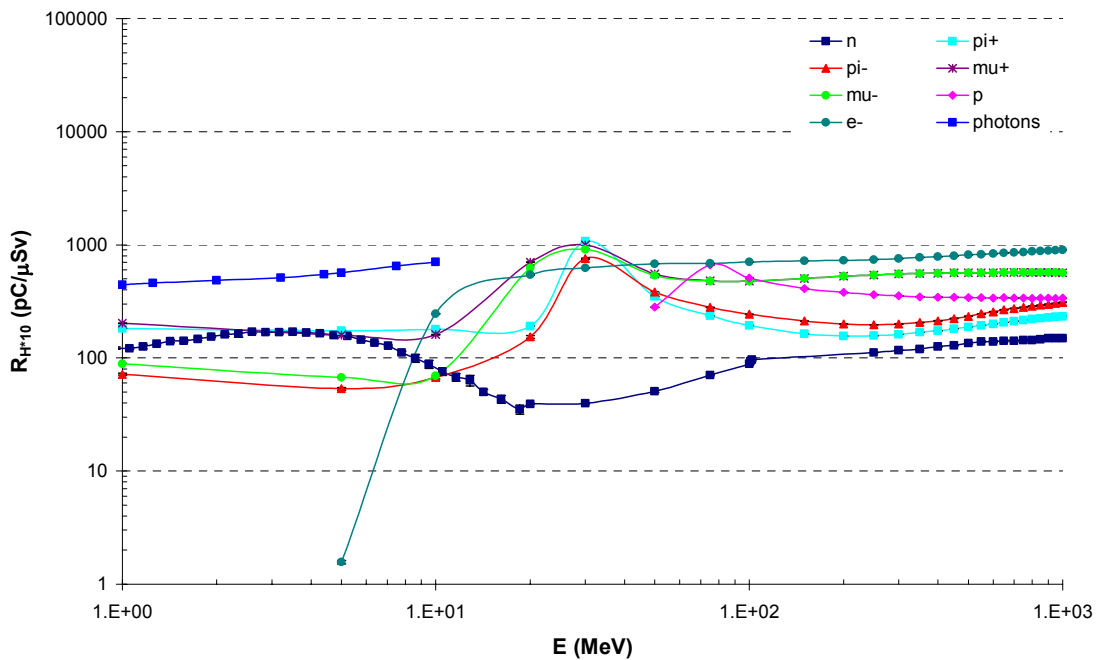


**Figure 14** Response functions for protons, neutrons, muons, charged pions and electrons expressed in terms of created charge per unit dose equivalent for a hydrogen-filled IG5 chamber. Conversion coefficients for electron energies below 2 MeV and for proton energies below 50 MeV were not available from [10].

## 6 ANGULAR DEPENDENCE OF THE RESPONSE

Due to the asymmetry of the chamber it is important for practical applications to study the angular dependence of the response of the monitor. First tests were performed at CERN and at the PSI [4] irradiating the devices under different angles  $\theta$ . In order to obtain a similar situation in the simulation a source was implemented and linked to FLUKA that allowed rotating the beam direction with respect to the monitor at an arbitrary angle.

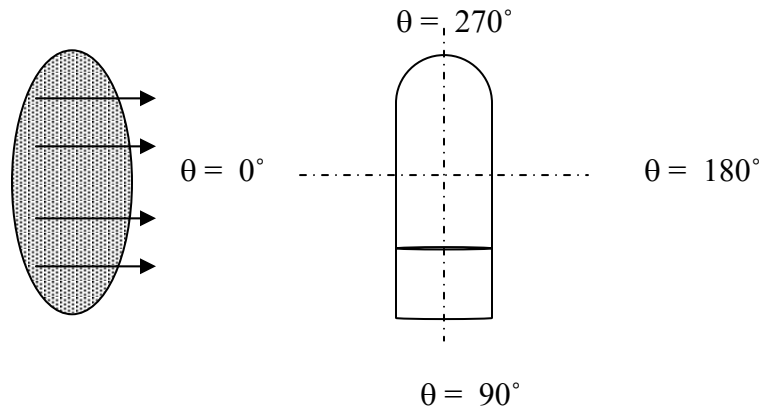


**Figure 15** Orientation of the beam direction with respect to the chamber. The angle  $\theta$  denotes the rotation angle of the chamber. It is counted counter clockwise with  $\theta = 0^\circ$  being lateral irradiation,  $\theta = 90^\circ$  irradiation of the rear of the chamber, etc.

In accordance with experimental studies [4] the angular dependence of the response to photons was calculated for both monitor types using the X-ray spectra N120, N300 as well as an energy of 660 keV of a Cs-137 source. Results for photons using both chamber types are illustrated in Figure 16 and 17. All values were normalised to the respective response for lateral irradiation ( $\theta = 0^\circ$ ).

As can be seen in Figure 16 and Figure 17 reasonable agreement within statistical uncertainties is obtained comparing simulated and measured responses for the X-ray spectra N120 and N300. On the other hand, deviations are found from the experimental values obtained with the Cs-137 source in the calibration laboratory at CERN. Possible reasons include scattering effects of the source encapsulation, the walls or the support of the chambers, which were not taken into account. Generally it is clearly visible that especially for low-energy photons the direction of the incoming radiation affects the response. In the case of irradiation of the rear of the monitor with respect to the beam directed towards the electronics box ( $\theta = 90^\circ$ ), one finds attenuation of the photon fluence that can be explained by the increased amount of material that has to be penetrated. Considering the situation of the beam traversing the chamber from the head a slight drop in the response is visible. This effect can also be explained by the slightly larger amount of shell and electrode material that has to be penetrated.

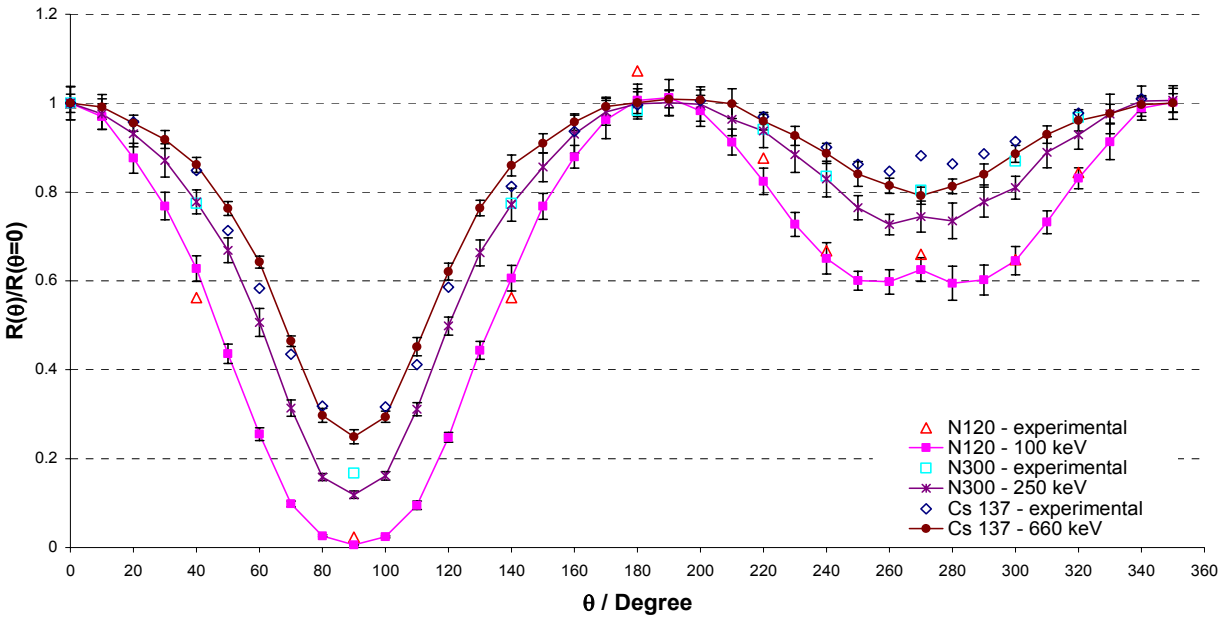


**Figure 16** Angular dependence of the response of an argon-filled IG5 chamber to photons of various energies. Values are normalized to the response at  $\theta=0^\circ$ . An angle of  $\theta=90^\circ$  denotes a beam orientation at which the monitor is irradiated from its rear (electronics box), whereas at  $\theta=270^\circ$  the beam is traversing the chamber from its head.

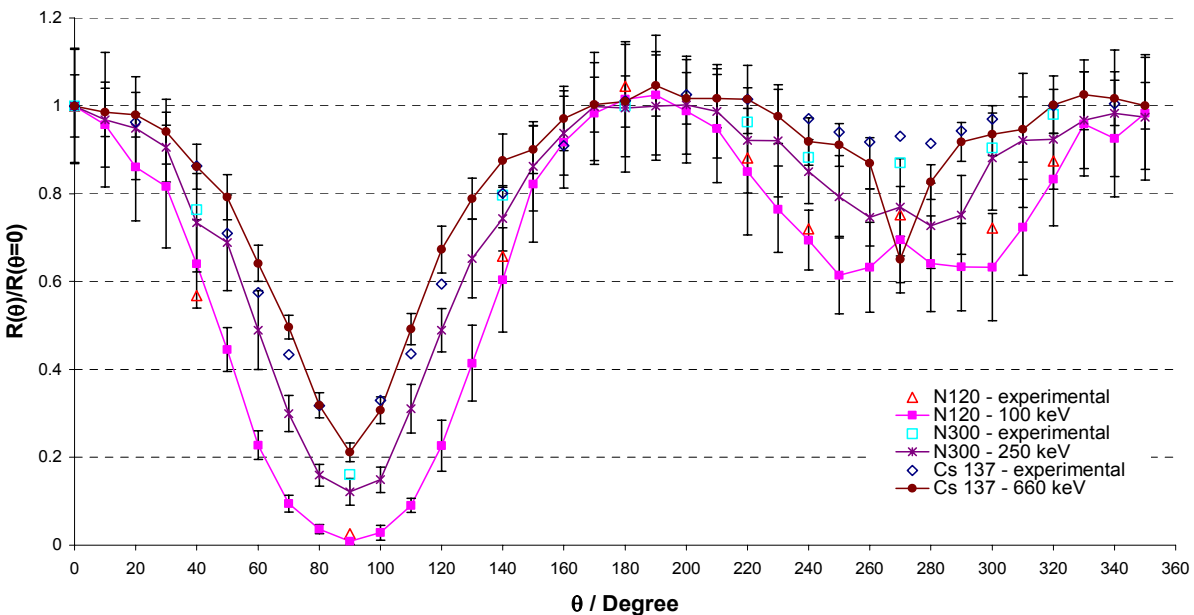


**Figure 17** Angular dependence of the response of a hydrogen-filled IG5 chamber to photons of various energies. Values are normalized to the response at  $\theta=0^\circ$ . An angle of  $\theta=90^\circ$  denotes a beam orientation at which the monitor is irradiated from its rear (electronics box), whereas at  $\theta=270^\circ$  the beam is traversing the chamber from its head.

Similar calculations were performed using neutrons of various energies and results are illustrated in Figure 18 and Figure 19. Again a decrease in the response of both monitor types can be observed for irradiation from the rear (electronics box) for energies of 5 MeV and 50 MeV. In the case of neutrons a shift in energy of the incident particles is caused by the larger amount of steel that has to be traversed. Taking into account that the response of an argon-filled and a hydrogen-filled chamber decreases, especially below 5 MeV (see Figure 6), the lower response can be understood. As can be seen in Figure 18 and Figure 19 at high energy the response for irradiation of the rear of the monitor is increased with respect to lateral irradiation. This effect is caused by hadronic cascades in the electronics box and the base plate, producing secondary particles which deposit energy in the active volume. In order to investigate the reason for the sharp drops that can be seen at exactly  $\theta = 90^\circ$ , the calculations were repeated with all materials set to vacuum with the exception of the active volume. It was found that these effects can be traced back to the material enclosing the active volume.

As illustrated in the Figure 18 and Figure 19, similar sharp drops for neutron energies of 50 MeV and 500 MeV can be observed for argon- and hydrogen-filled monitors at exactly  $\theta = 270^\circ$ . In contrast to this at 5 MeV only a relatively small decrease in the response can be observed for an argon-filled device, whereas an increase in the response of a hydrogen-filled chamber is visible. Performing simulations with all materials set to vacuum, with the exception of the active volume, showed that the diminution of the response for this specific chamber orientation can be attributed to effects of the shell material, whereas the increase of the response for a hydrogen-filled chamber at 5 MeV persists. Consequently this effect originates from the active medium and can be explained by the fact that, in contrast to lateral irradiation, the secondary particles might cover a longer distance in the active volume due to scattering mostly in forward direction, which results in higher interaction probability.

**Table 5** Results of the simulation and the measurements of the response to neutrons as a function of the angle  $\theta$  normalized to the response at  $\theta = 0^\circ$ .

Energy [MeV]	Angle $\theta$ [degrees]	Ar - Ratio (experiment)	Ar - Ratio (simulation)	H - Ratio (experiment)	H - Ratio (simulation)
<b>0.565</b>	0	1.00 ± 7.46 %	1.00 ± 2.63 %	1.00 ± 1.76 %	1.00 ± 0.57 %
	90	0.45 ± 9.11 %	0.41 ± 7.71 %	0.43 ± 1.97 %	0.41 ± 1.12 %
	270	0.86 ± 8.44 %	1.00 ± 3.72 %	0.95 ± 5.43 %	0.86 ± 0.84 %
<b>1.2</b>	0	1.00 ± 4.14 %	1.00 ± 2.73 %	1.00 ± 3.93 %	1.00 ± 0.60 %
	90	0.65 ± 5.89 %	0.46 ± 3.43 %	0.48 ± 4.59 %	0.48 ± 1.90 %
	270	0.94 ± 5.78 %	1.00 ± 3.86 %	0.96 ± 4.48 %	0.91 ± 1.13 %
<b>2.5</b>	0	1.00 ± 4.72 %	1.00 ± 2.29 %	1.00 ± 2.62 %	1.00 ± 1.34 %
	90	0.57 ± 5.62 %	0.43 ± 2.65 %	0.52 ± 3.30 %	0.46 ± 1.48 %
	270	0.72 ± 6.16 %	1.00 ± 3.24 %	0.98 ± 3.27 %	0.92 ± 2.27 %
<b>5.0</b>	0	1.00 ± 1.80 %	1.00 ± 0.87 %	1.00 ± 1.80 %	1.00 ± 0.87 %
	90	0.61 ± 2.07 %	0.48 ± 1.87 %	0.61 ± 2.07 %	0.48 ± 1.87 %
	270	0.84 ± 6.33 %	1.00 ± 1.23 %	0.84 ± 6.33 %	1.00 ± 1.23 %
<b>14.8</b>	0	1.00 ± 4.39 %	1.00 ± 0.37 %	1.00 ± 4.39 %	1.00 ± 0.37 %
	90	0.67 ± 4.42 %	0.54 ± 1.09 %	0.67 ± 4.42 %	0.54 ± 1.09 %
	270	0.90 ± 4.46 %	1.00 ± 0.53 %	0.90 ± 4.46 %	1.00 ± 0.53 %

As can be seen from Table 5 reasonable agreement was found for the experimental and the simulated results.

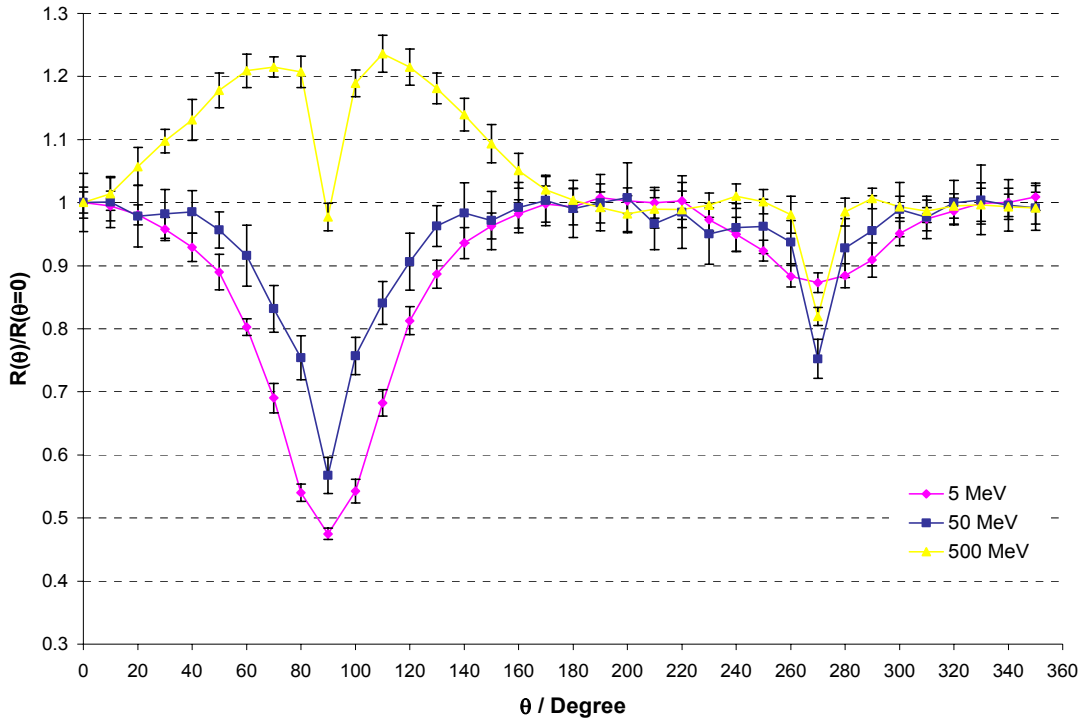


**Figure 18** Angular dependence of the response of an argon-filled IG5 chamber to neutrons of various energies. Values are normalized to the response at  $\theta = 0^\circ$ .

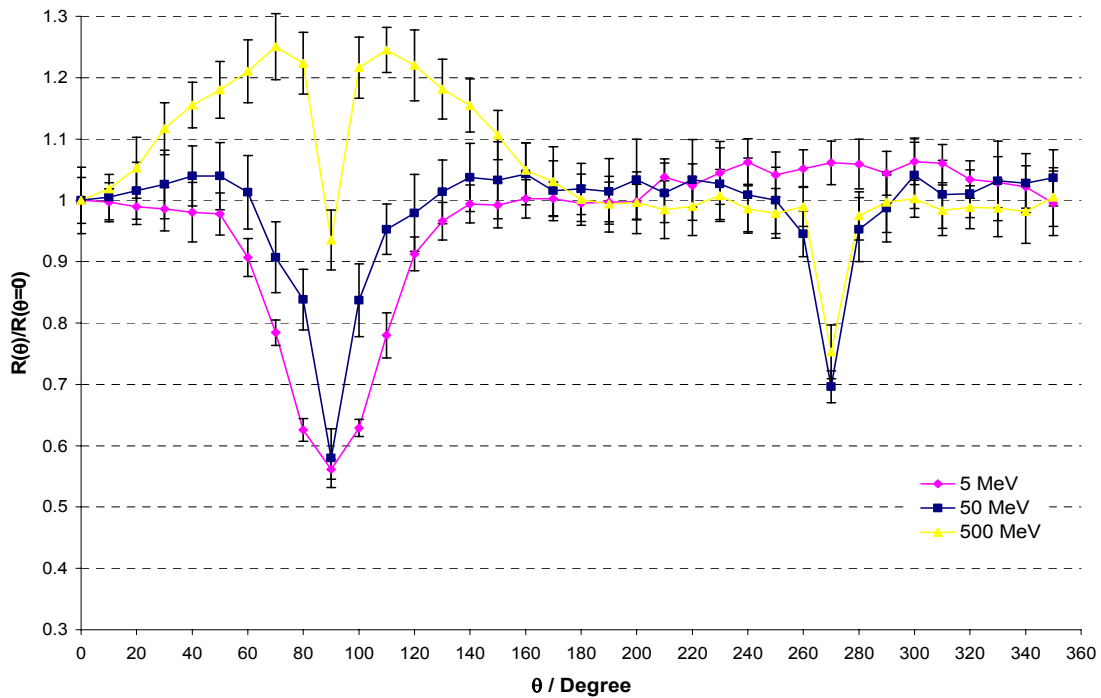


**Figure 19** Angular dependence of the response of a hydrogen-filled IG5 chamber to neutrons of various energies. Values are normalized to the response at  $\theta = 0^\circ$ .

## 7 RESULTS & CONCLUSIONS

The response of an argon- and a hydrogen-filled ionisation chamber as function of energy and particle type was studied with detailed Monte Carlo simulations and verified for photons and neutrons in calibration measurements. For both IG5 chamber types the respective response to photons, neutrons, protons, muons, charged pions and electrons has been studied. As a result it was found that the argon-filled monitors, as expected, show a response to photons which is higher by the order of a magnitude, than that of the hydrogen-filled-chambers. For both devices comparisons to calibration measurements have been carried out, which showed good agreement. The same calculations have been performed for proton, muon, charged pion and electron irradiation.

Calculations for neutron irradiation showed generally that considering low-energy neutrons in the range from 1 keV to 15 MeV, the hydrogen-filled monitor is much more sensitive. However, above 100 MeV the onset of spallation reactions in argon cause the response of the argon-filled chamber to exceed that of the hydrogen-filled monitor. The conclusion that therefore argon-filled monitors are better suited for the detection of high energy neutrons should be made with care only. It is important to keep in mind that the sensitivity to charged particles and photons that might originate from background radiation is higher as well. Experimental verification of the calculated response functions showed good agreement in general for hydrogen-filled chambers. In the case of the argon-filled chamber large deviations were found. These discrepancies are not yet fully understood but it is important to keep in mind that in principle the calculated and the measured quantity are different. As a result of the FLUKA simulation one obtains energy deposition which for argon is based on kerma factors, whereas for hydrogen detailed kinematics of elastic scattering on hydrogen nuclei and the transport of recoil protons are implemented. Furthermore the assumption of an energy-independent  $W$ -factor might also contribute to possible deviations in the comparison to the measured quantity, which is the charge created in the active volume. Further investigations of this matter have to be performed.

Furthermore, the angular dependence of the response of the chambers has been studied for photon and neutron irradiation. A significant decrease in the response was found for irradiation of the rear of the chamber and low energies, which is due to attenuation by the base plate. On the other hand, for high-energy neutrons of 500 MeV an increase in the response was observed, because induction of hadronic cascades causes more energy to be deposited within the active volume. Measurements of the angular dependence of the response with respect to lateral irradiation were performed in neutron calibration fields of various energies. For both chamber types the results showed good agreement in comparison to the calculations.

In order to verify the simulated response functions, it is necessary to test both monitor types in a mixed radiation field of known particle and energy composition. Based on the calculated response functions and the available particle spectra it should be possible to determine the amount of charge created within the respective active volume. This charge can be compared directly to the experimental value to validate the results for mixed radiation fields. First experiments in such fields have been performed at the CERN-EU

high-energy Reference Field (CERF). The results obtained are currently subject to analysis and not yet ready.

### **Acknowledgements**

We would like to thank Thomas Otto for discussions and generously providing the FLUKA input and the results of his preliminary studies. In addition we would also like to thank Doris Forkel-Wirth for stimulating discussions.

## References

- 1 A. Fassò, A.Ferrari, P.R. Sala, *Electron-photon transport in FLUKA: status*, Proceedings of the MonteCarlo 2000 Conference, Lisbon, October 23-26 2000, A.Kling, F.Barao, M.Nakagawa, L.Tavora, P.Vaz - eds., Springer-Verlag Berlin, p.159-164 (2001)
- 2 A. Fassò, A. Ferrari, J. Ranft, P. R. Sala, *FLUKA: Status and Prospective for Hadronic Applications*, Proceedings of the MonteCarlo 2000 Conference, Lisbon, October 23-26 2000, A.Kling, F.Barao, M.Nakagawa, L.Tavora, P.Vaz - eds. , Springer-Verlag Berlin, p.955-960 (2001)
- 3 T. Otto, *Preliminary simulation results for the sensitivity of Centronic high-pressure ionisation chambers*, CERN Technical Note TIS-RP-TN-2002-011 (2002)
- 4 A. Hess, *Détermination de la réponse de chambres d'ionisation prévues pour la surveillance du LHC*, CERN/Haute Ecole Specialisee du Suisse Occidentale (2002)
- 5 A. Mitaroff, M. Silari, *The CERN-EU high-energy Reference Field (CERF) facility for dosimetry at commercial flight altitudes and in space*, Radiation Protection Dosimetry 102(1), pp. 7-22 (2002)
- 6 Material Property Data, [www.matweb.com](http://www.matweb.com)
- 7 International Commission on Radiation Units and Measurements, *Average Energy Required To Produce An Ion Pair*, ICRU Report 31, Washington D.C. (1979)
- 8 G. F. Knoll, *Radiation Detection and Measurement*, 3<sup>rd</sup> Edition, Wiley & Sons (1999)
- 9 International Commission for Radiological Protection, *Conversion Coefficients for Use in Radiological Protection*, (ICRP 74) Pergamon Press, Oxford (UK), (1997)
- 10 M. Pelliccioni, *Overview of Fluence-to-Effective Dose and Fluence-to-Ambient Dose Equivalent Conversion Coefficients for High Energy Radiation Calculated Using the FLUKA Code*, Radiation Protection Dosimetry 88(4), pp. 279-297 (2000)
- 11 U. Ankerhold, *Catalogue of X-ray spectra and their characteristic data – ISO and DIN radiation qualities, therapy and diagnostic radiation qualities, unfiltered X-ray spectra*, PTB Bericht PTB-Dos-34 (2000)
- 12 H. J. Brede *et al.*, *The Braunschweig accelerator facility for fast neutron research*, Nuclear Instruments and Methods, pp. 349-358 (1980)



## APPENDIX

### Conversion factors

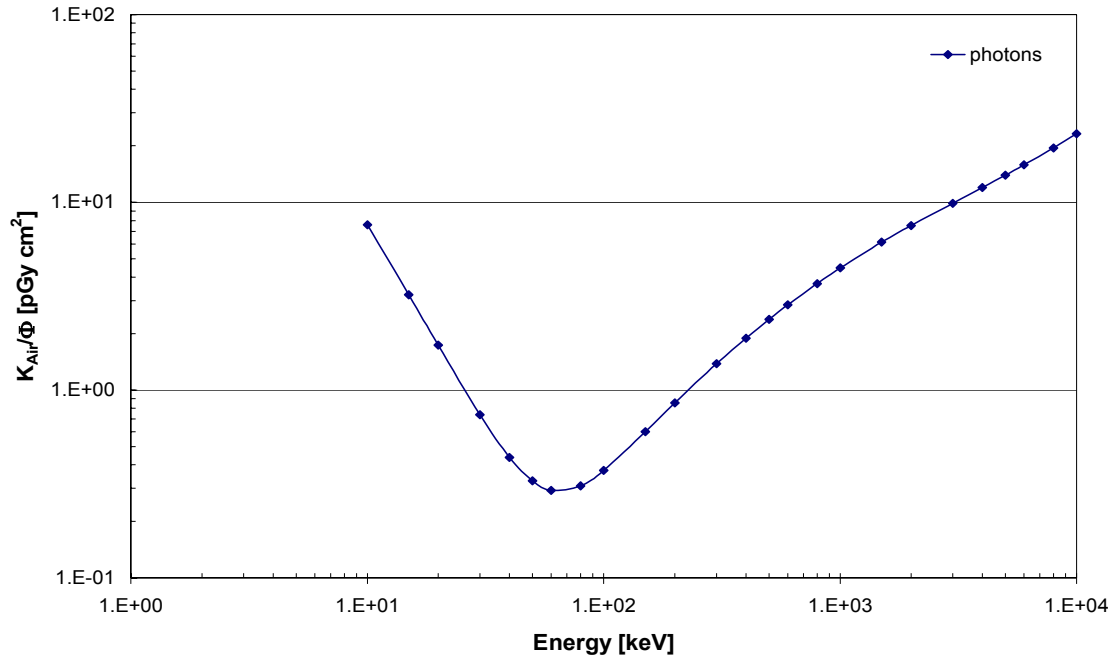


Figure 20 Conversion coefficients from photon fluence to kerma free-in-air [9].

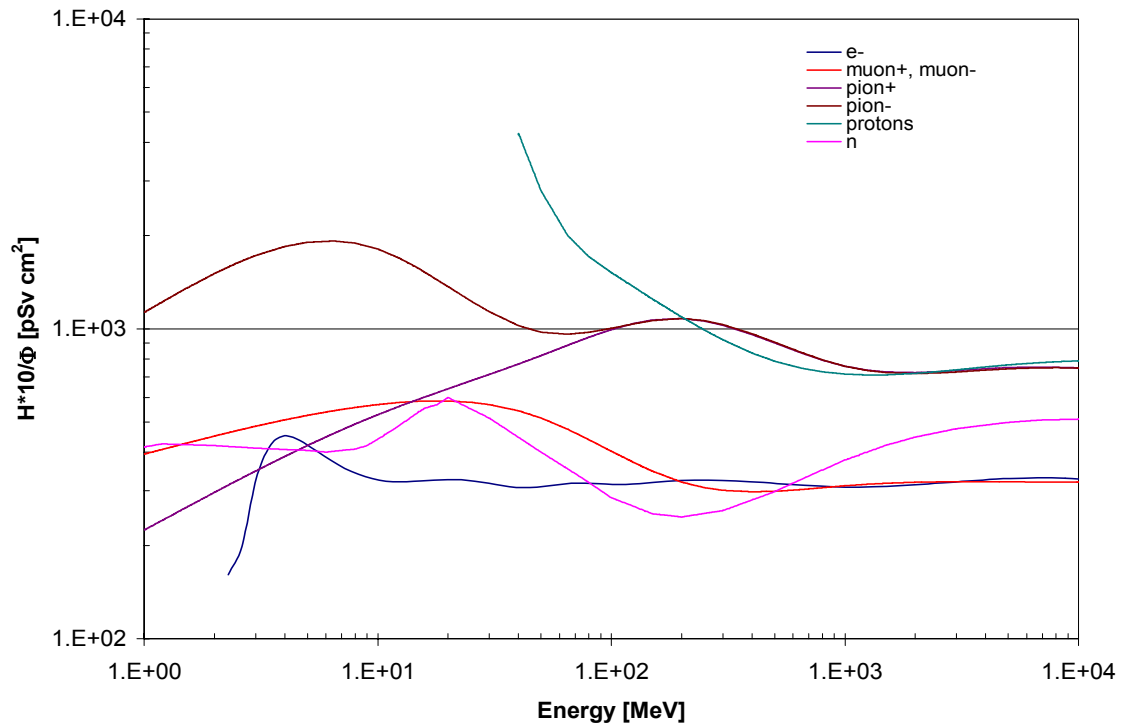


Figure 21 Conversion factors from fluence to ambient dose equivalent given for neutrons, protons, electrons, charged pions and muons [10].